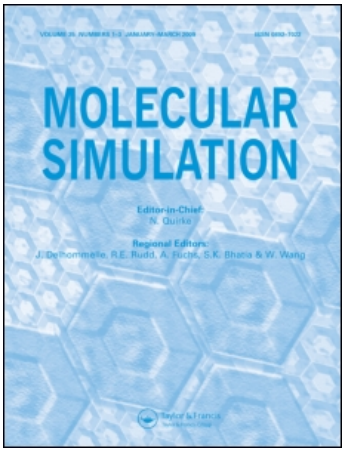

Molecular Simulation
Publication details, including instructions for authors and subscription information:
http://www.informaworld.com/smpp/title~content=t713644482

Molecular dynamics study of methane in water: diffusion and structure

J. Zhang[a]; S. Piana[b]; R. Freij-Ayoub[c]; M. Rivero[c]; S. K. Choi[a]
[a] CSIRO Petroleum, South Clayton, Vic., Australia [b] Nanochemistry Research Institute, Curtin University of Technology, Perth, WA, Australia [c] CSIRO Petroleum, Bentley, WA, Australia

To cite this Article Zhang, J. , Piana, S. , Freij-Ayoub, R. , Rivero, M. and Choi, S. K.(2006) 'Molecular dynamics study of methane in water: diffusion and structure', Molecular Simulation, 32: 15, 1279 — 1286
To link to this Article: DOI: 10.1080/08927020601039598
URL: http://dx.doi.org/10.1080/08927020601039598

Molecular Simulation, Vol. 32, No. 15, 30 December 2006, 1279–1286

Molecular dynamics study of methane in water: diffusion and structure

J. ZHANG†*, S. PIANA‡§, R. FREIJ-AYOUB¶‖, M. RIVERO¶# and S. K. CHOI†**

†CSIRO Petroleum, Private Bag 10, South Clayton, Vic. 3169, Australia
‡Nanochemistry Research Institute, Curtin University of Technology, GPO Box U1987, Perth, WA, 6845, Australia
¶CSIRO Petroleum, P.O. Box 1130, Bentley, WA, 6102, Australia

(Received August 2006; in final form September 2006)

We present molecular dynamics simulation results for the diffusion coefficients and structure of water–methane mixtures in constant NPT ensembles, at $T = 270$, 300 K and $P = 8.104 \times 10^7$ Pa. The systems we have studied consist of one, four and eight CH_4 molecules and varying H_2O molecules per unit cell, which correspond to methane concentration of 0.081, 0.324 and 0.643 mol/l, respectively. The intermolecular potentials used in all the simulations were the four-site TIP4P model of water [1] and the fitted Lennard-Jones 12-6 potential for CH_4—H_2O [2]. Our results show that the methane concentration has little impact on the structure of water and the formation of hydrogen bonds (H-bonds) between water molecules. The H-bond numbers, H-bond length and the H-bond angle are independent of the methane concentration at the temperatures and densities examined in this study. We also find that the number of H-bonds and angles are sensitive to the temperature. The rise of temperature produces a decrease in the number and an increase in the angle of the H-bonds. Enhanced structuring of the hydration-shell water molecules is indicated by an increase of the first and second peak in the water oxygen–oxygen radial distribution function as temperature is decreased. The self-diffusion coefficient of water is sensitive to the methane concentration and temperature.

Keywords: Methane hydrate; Molecular dynamics simulation; Hydrogen bond; Methane concentration

1. Introduction

Clathrate hydrates are a class of solids in which gas molecules occupy "cages" made up of hydrogen-bonded water molecules. They are of an immediate and practical concern, due to the hazards they pose to oil and gas drilling and production operations. The formation of gas hydrate under certain temperature and pressure conditions can cause costly and hazardous blockage of natural gas pipelines. Many components of natural gas form gas hydrates at low temperatures and elevated pressure. There are three types of gas hydrate structures. These structures differ in the number and sizes of the cages and in their unit cells. The type of the gas hydrate depends on the size of the guest molecules ranging from noble gas atoms to large organic molecules. All these hydrate structures consist of two or more types of water cages packed within the crystal lattice. Most of the previous research on natural gas hydrate formation is focused on the equilibrium properties of gas hydrates, such as pressure measurements as a function of temperature and gas consumption versus temperature. Methane gas hydrate studies have recently attracted attention due to their importance for significant natural resource [3–7]. Skipper has performed molecular dynamics simulation to study the aggregation of simple apolar particles in aqueous solution as a function of temperature [8]. Chau and Mancera have performed Monte Carlo simulations to investigate the effect of pressure on the structural properties of the water molecules hydrating methane [9]. Mancera and Buckingham have carried out a series of NVE molecular dynamics simulations of ethane in water at different temperatures near room temperature to try to obtain a clear picture of the molecular mechanisms

*Corresponding author. Tel.: + 61-3-9545-8358. Fax: + 61-3-9545-8380. Email: junfang.zhang@csiro.au
§Tel.: +61-8-9266-2687. Email: piana@power.curtin.edu.au
‖Tel.: +61-8-6436-8631. Email: reem.freij-ayoub@csiro.au
#Tel.: +61 8 6436 8753. Email: mayela.rivero@csiro.au
**Tel.: +61-3-9545-8391. Fax: +61-3-9545-8380. Email: xavier.choi@csiro.au

Molecular Simulation
ISSN 0892-7022 print/ISSN 1029-0435 online © 2006 Taylor & Francis
http://www.tandf.co.uk/journals
DOI: 10.1080/08927020601039598

Table 1. Thermodynamic properties for the simulations.

Number of molecules	*Temperature (K)*	*U(KJ/mol)*	*u(KJ/mol)*	*Density(g/cm^3)*
$NCH_4 = 1$	270	-26064 ± 98	-36.76 ± 0.13	1.040 ± 0.005
NWATER = 708	300	-24237 ± 95	-34.18 ± 0.13	1.027 ± 0.005
$NCH_4 = 4$	270	-25994 ± 103	-36.66 ± 0.14	1.031 ± 0.005
NWATER = 705	300	-24159 ± 95	-34.07 ± 0.13	1.019 ± 0.005
$NCH_4 = 8$	270	-26046 ± 105	-36.53 ± 0.13	1.021 ± 0.005
NWATER = 705	300	-24177 ± 101	-33.90 ± 0.14	1.007 ± 0.005

NCH_4 is the number of methane molecules and NWATER is the number of water molecules in the simulation box. *U* is the internal energy and *u* the internal energy per water molecule. The rms deviation values are shown after the average.

responsible for the effect of temperature on the hydration structure [19].

However, to the best of our knowledge, there have been a limited number of molecular dynamics and Monte Carlo investigations into the effect of methane concentration and temperature on the hydration structure, the hydrogen bond (H-bond) network and transport properties. In this paper we present molecular dynamics simulation results of the diffusion coefficient and hydration structure for the systems of water–methane mixtures with two different temperatures and three methane concentrations in constant NPT ensembles. The remainder of this paper is structured as follows. In Section 2 we explain simulation details. In Section 3 the results and discussions are presented and finally our analysis is summarized and concluded in Section 4.

2. Simulation details

In this study, the molecular dynamics simulations were performed using GROMACS [10–12]. The systems we have studied consist of one, four and eight CH_4 molecules and varying H_2O molecules per unit cell, which correspond to methane concentration of 0.081, 0.324 and 0.643 mol/l, respectively. The intermolecular potentials used in all the simulations were the four-site TIP4P model of water [1] and the fitted Lennard-Jones 12-6 potential for CH_4—H_2O [2]. Force calculations were truncated at a distance of 0.9 nm. For the calculation of long-range electrostatic forces, particle-mesh Ewald (PME) method proposed by Darden [13,14] was used. All bond lengths were constrained using the Shake algorithm [15] with a geometric tolerance of 0.0001. The temperature was fixed

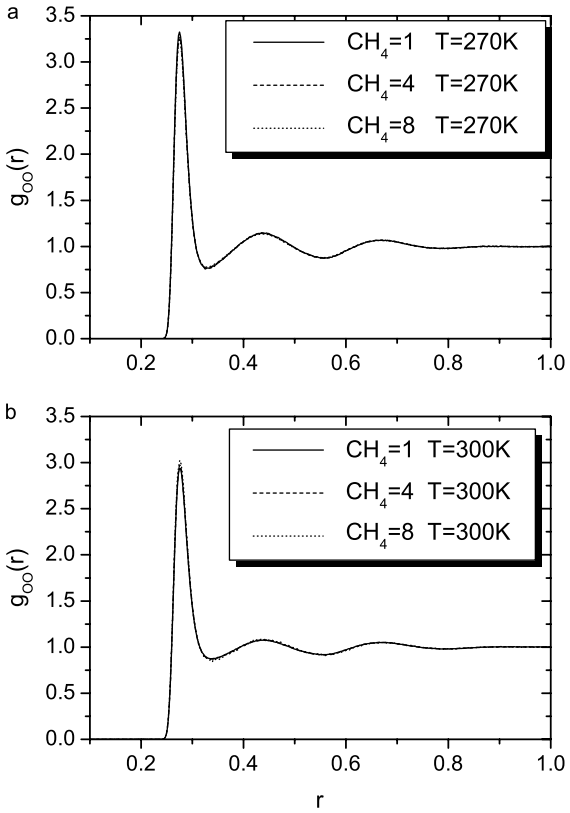

Figure 1. Oxygen–oxygen radial distribution function (O—O RDF) for the systems of different methane concentrations. (a) $T = 270$ K; (b) $T = 300$ K.

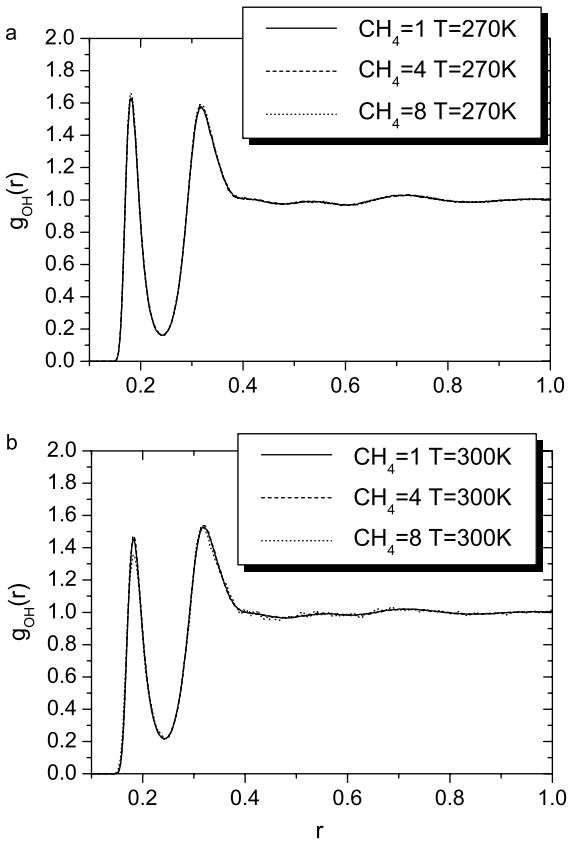

Figure 2. Oxygen–hydrogen radial distribution function (O—H RDF) for the systems of different methane concentrations. (a) $T = 270$ K; (b) $T = 300$ K.

by using Berendsen thermostat [16] at 270 and 300 K, and the Berendsen pressure coupling algorithm was used to keep the pressure constant.

Periodic boundary conditions were applied in three directions. The equations of motion were integrated with a 1 fs time step. The initialization of each MD run was done in two steps. The first step consisted of a 5-ps simulation with the steepest-descent method to perform energy minimization in order to reduce the thermal noise in the structures and potential energies. The second step consisted of a 1-ns simulation at the same temperature to reach equilibrium configurations before statistical averages were taken. Once equilibrium was achieved, production runs of a total of 5×10^6 time steps (5 ns) were carried out.

3. Results and discussion

Table 1 shows the thermodynamic properties of the simulations. As expected, for each methane concentration value, the increase in temperature produces an increase in internal energy as the density decreases.

3.1 Radial distribution functions

The structure of water in the water–methane mixtures is described by O—O, O—H and H—H radial distribution functions. Figure 1 shows the O—O radial distribution function, $g_{OO}(r)$, for the systems of different methane concentrations at temperature 270 K (figure 1(a)) and 300 K (figure 1(b)). It can be seen that $g_{OO}(r)$ is barely distinguishable between the systems with different methane concentrations. A similar situation has been observed in O—H and H—H radial distribution functions in figures 2 and 3. This suggests that the methane concentration has little impact on the structure of water and the tendency to form H-bonds between water molecules.

The effect of temperature on the radial distribution function, $g_{OO}(r)$, $g_{OH}(r)$ and $g_{HH}(r)$ for the systems of different methane concentrations is shown in figures 4–6, respectively. It can be seen from these figures that the first and second peaks of $g_{OO}(r)$, $g_{OH}(r)$ and $g_{HH}(r)$ reduce in height as the temperature is increased from 270 to 300 K, indicating that water becomes less structured as

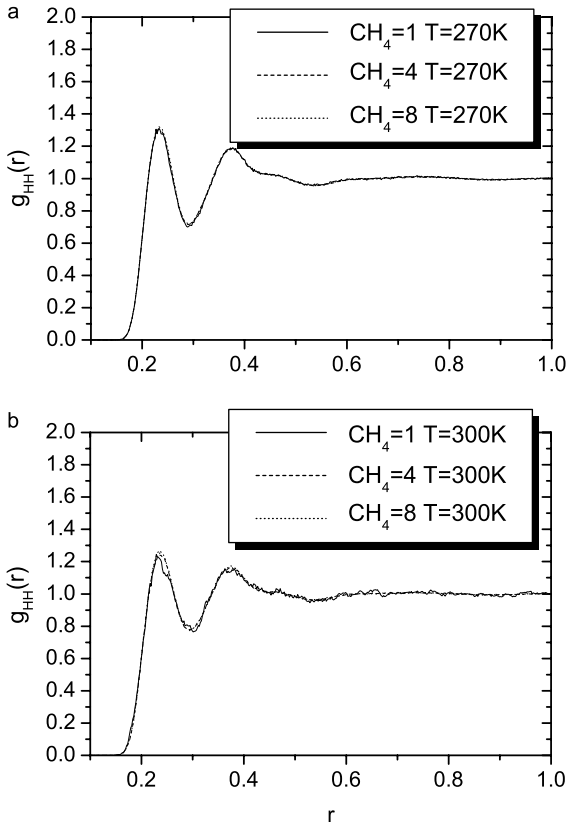

Figure 3. Hydrogen–hydrogen radial distribution function (H—H RDF) for the systems of different methane concentrations. (a) $T = 270$ K; (b) $T = 300$ K.

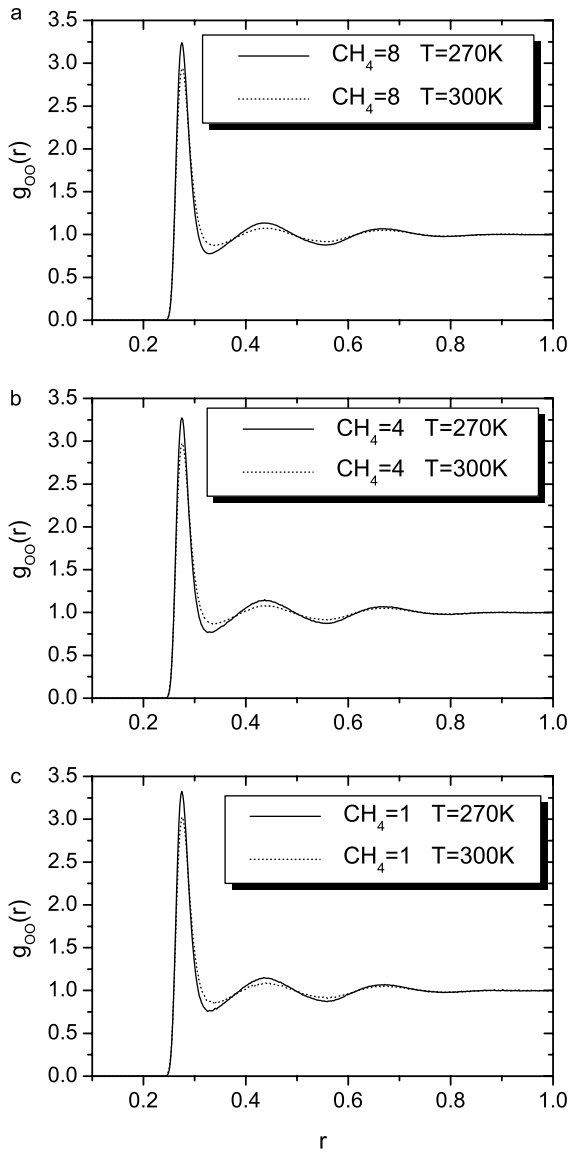

Figure 4. Comparison of oxygen–oxygen radial distribution function (O—O RDF) for the systems at temperature 270 and 300 K, with methane concentration of (a) 0.643 mol/l; (b) 0.324 mol/l; (c) 0.081 mol/l.

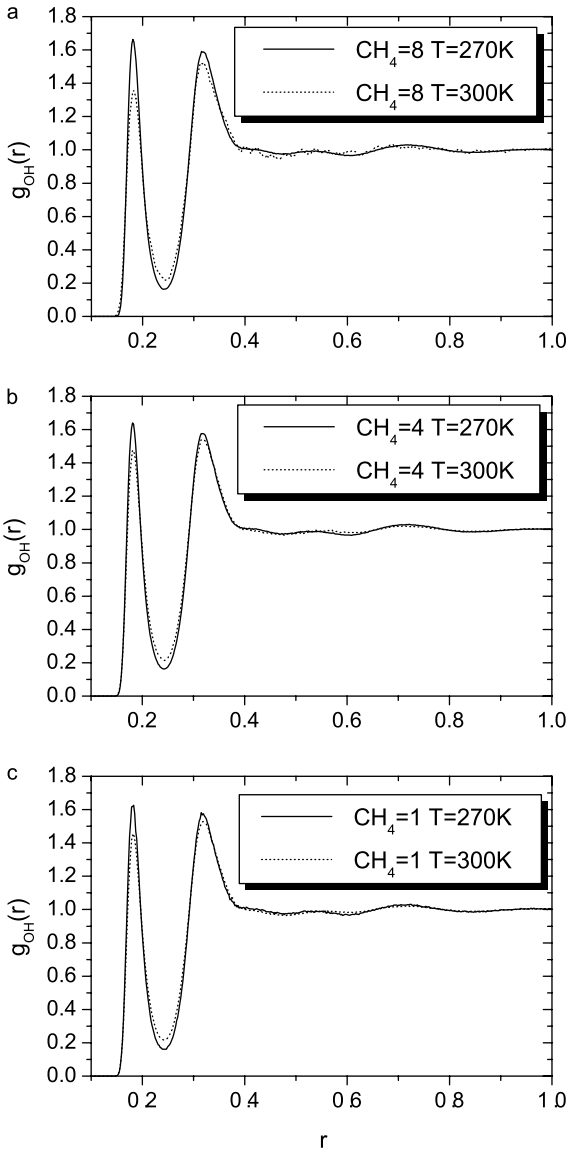

Figure 5. Comparison of oxygen–hydrogen radial distribution function (O—H RDF) for the systems at temperature 270 and 300 K, with methane concentration of (a) 0.643 mol/l; (b) 0.324 mol/l; (c) 0.081 mol/l.

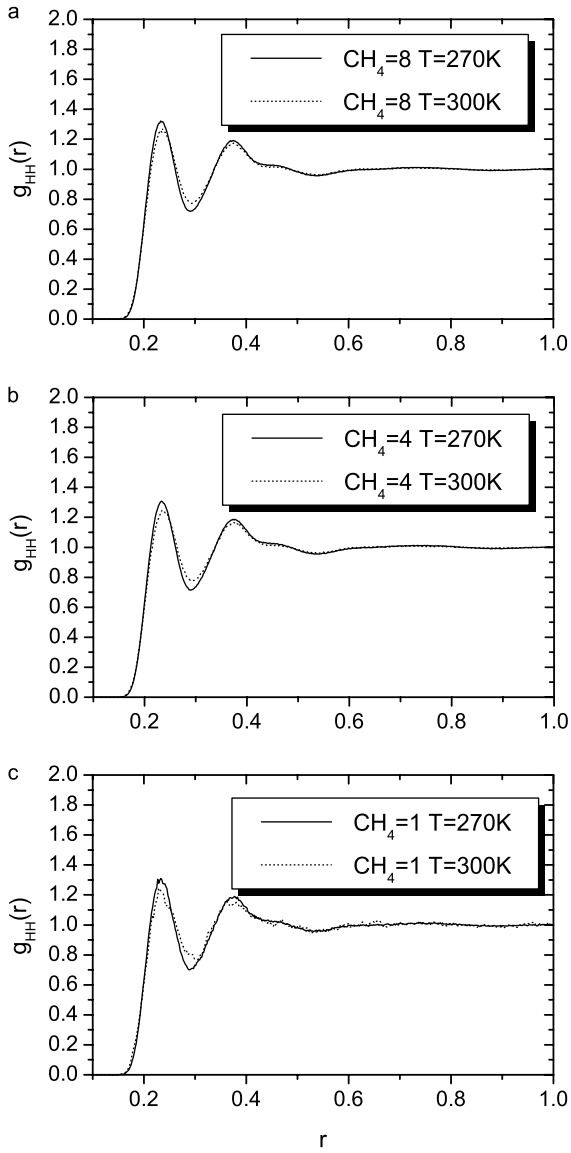

Figure 6. Comparison of hydrogen–hydrogen radial distribution function (H—H RDF) for the systems at temperature 270 and 300 K, with methane concentration of (a) 0.643 mol/l; (b) 0.324 mol/l; (c) 0.081 mol/l.

temperature is increased under our simulation conditions. The systems of different methane concentrations demonstrate the similar behaviour in the temperature dependence of the radial distribution functions. We observe $g_{OO}(r)$ in figures 1 and 4, has a first peak at 2.75 Å, with the second nearest-neighbour O—O pair correlations occurring at around 4.40 Å and the third one at 6.67 Å. Water has the strong tendency to form linear H-bonds. $g_{OH}(r)$ in figures 2 and 5 shows the first peak at 1.81 Å, which corresponds to the average length of the H-bonds between water molecules. The experimental H-bond [17] between bulk water molecules is 1.85 Å. H—H correlation at 2.38 Å can be seen in figures 3 and 6. Figure 7 shows the comparison of methane–methane radial distribution function (CH_4—CH_4 RDF) for the systems at temperature 270 and 300 K, with methane concentration of 0.643 and 0.324 mol/l. As the temperature is increased from 270 to 300 K, we observe an increasing tendency for methane molecules to come into direct contact. There is a noticeable peak at around 7.5 Å, corresponding to solvent separated pairs. Our data is consistent with the MD results reported in Ref. [8]. Figures 8 and 9 show the comparison of methane–oxygen and methane–hydrogen radial distribution function for the same systems described above. We consider the 300 K results of our work. The methane–oxygen first maximum attains a value of 1.8 at 3.8 Å, while the first minimum has a value of 0.74 at 5.5 Å. For the methane–hydrogen, we obtain a first maximum value of 1.38 at 3.8 Å, while the first minimum reaches 0.8 at 5.85 Å. Chau and Manceera [9] carried out a number of Monte-Carlo simulations of one methane solute in 499 water molecules at six different pressures and constant temperature 320 K. They reported a methane–oxygen first maximum of 1.43 at 3.73 Å and a first minimum of 0.75 at 5.4 Å; the methane–hydrogen first maximum of 1.09 at

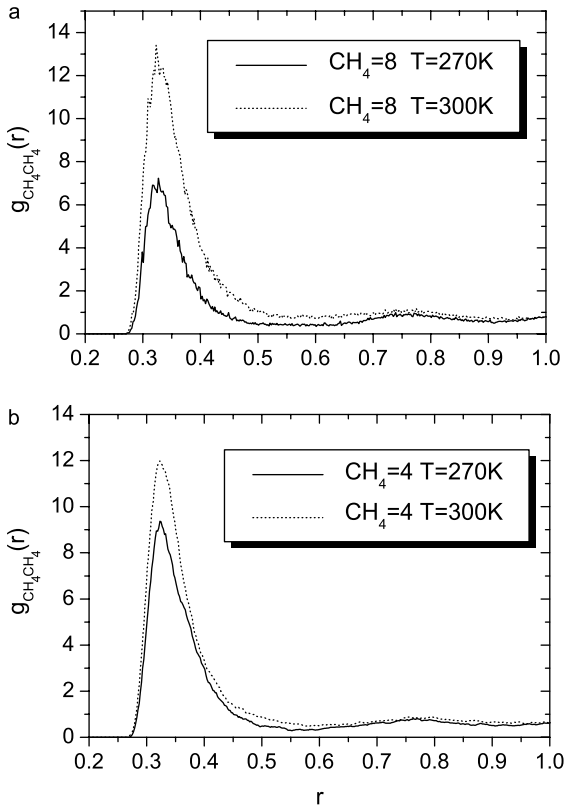

Figure 7. Comparison of methane–methane radial distribution function (CH_4—CH_4 RDF) for the systems at temperature 270 and 300 K, with methane concentration of (a) 0.643 mol/l; (b) 0.324 mol/l.

3.98 Å while the first minimum of 0.89 at 5.8 Å. Skipper [18] performed molecular dynamics simulations for the system of four methane molecules in 256 water molecules at three different temperatures, but at constant density. At 317 K, he reported a methane–oxygen first maximum of 2.0 at 3.5 Å and a first minimum of 0.75 at 5.3 Å; the methane–hydrogen first maximum of 1.4 at 3.5 Å while the first minimum of 0.8 at 5.7 Å. Our first maximum values of methane–oxygen and methane–hydrogen are between those reported by Chau and Manceera [9] and Skipper [18]. The difference can be caused by the different temperatures and the densities of the systems studied. As the temperature increases, the first maximum in both methane–oxygen and methane–hydrogen decrease and we can also discern a slight decrease in the second maximum. We can conclude by what we have observed that hydration structure is sensitive to the temperature under our simulation conditions.

3.2 Hydrogen bonds

The H-bonds between all possible donors and acceptors were analyzed. H-bonds are determined based on cutoffs for the angle, hydrogen—donor–acceptor (30°), and the distance of the donor–acceptor (3.5 Å). To determine if an H-bond exists, a geometrical criterion is used: water molecules were considered to be near neighbors if their oxygens were not more than 3.5 Å apart. The value 3.5 Å corresponds to the first minimum of the oxygen–oxygen

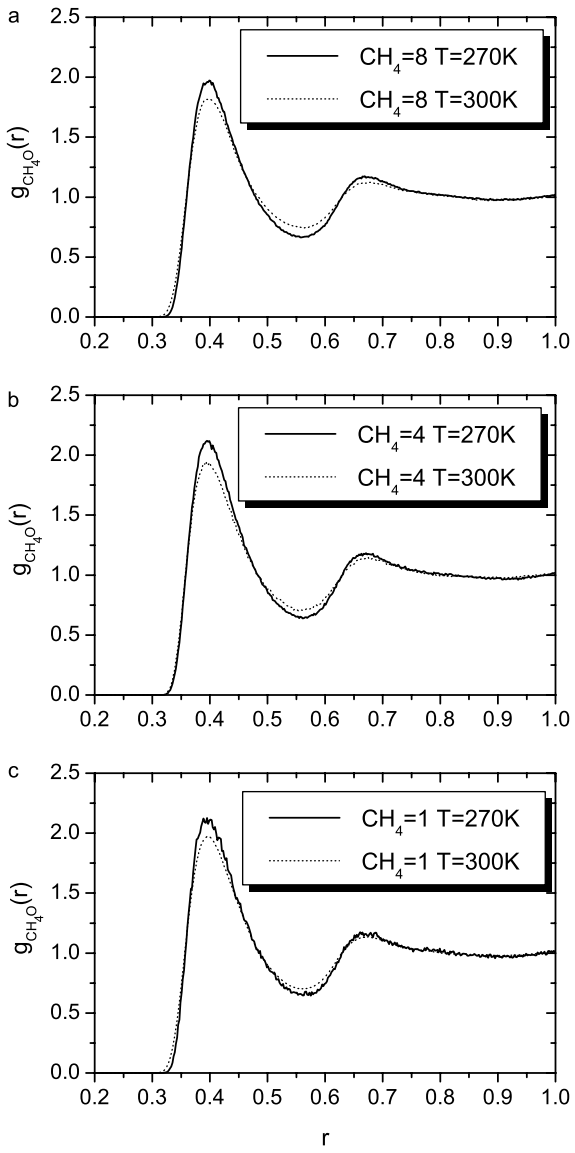

Figure 8. Comparison of methane–oxygen radial distribution function (CH_4—O RDF) for the systems at temperature 270 and 300 K, with methane concentration of (a) 0.643 mol/l; (b) 0.324 mol/l; (c) 0.081 mol/l.

radial distribution function of water. The angle, hydrogen—donor–acceptor, should not be larger than 30°. A H-bond angle was defined as the angle of hydrogen—donor–acceptor. Figure 10(a)–(c) show the comparison of the H-bond number distribution function for the systems at temperature 270 and 300 K, with methane concentration of 0.643, 0.324 and 0.081 mol/l, respectively. We observed that the number of H-bonds decreases with increasing temperature. When the temperature is increased, some H-bonds are broken due to larger thermal fluctuations that make the number of H-bonds decrease. Our results are in agreement with those of pair correlation functions indicating that the first and second peaks decrease as temperature is increased from 270 to 300 K, shown in figure 5, given in the previous section. Comparison of figure 10(a)–(c) shows that the number of H-bonds is remarkably insensitive to the methane concentration at the temperatures and densities examined in this study.

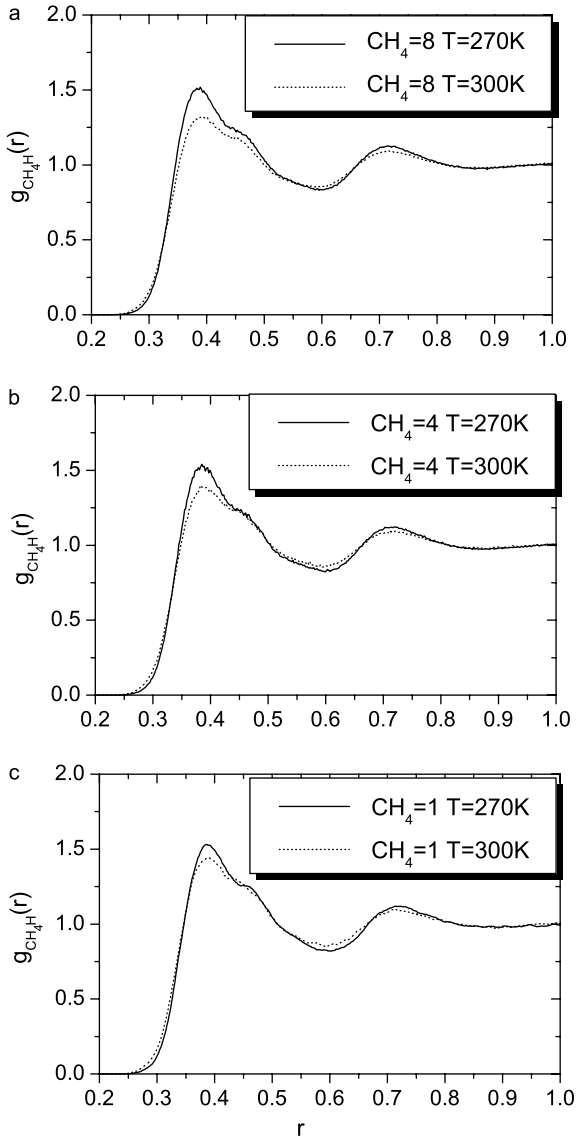

Figure 9. Comparison of methane– hydrogen radial distribution function (CH_4—H RDF) for the systems at temperature 270 and 300 K, with methane concentration of (a) 0.643 mol/l; (b) 0.324 mol/l; (c) 0.081 mol/l.

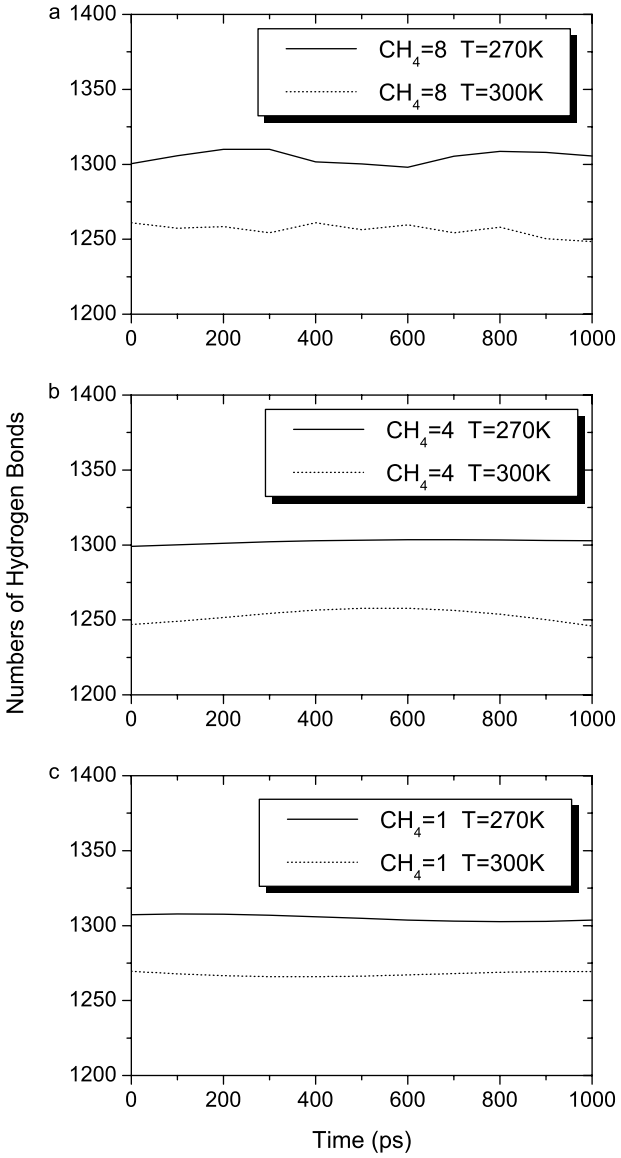

Figure 10. Comparison of the H-bond number distribution function for the systems at temperature 270 and 300 K, with methane concentration of (a) 0.643 mol/l; (b) 0.324 mol/l; (c) 0.081 mol/l.

In figure 11(a)–(c) we plot the donor–acceptor distance distribution of all H-bonds for the systems at temperature 270 and 300 K, with methane concentration of 0.643, 0.324 and 0.081 mol/l, respectively. We noticed that as temperature increases there is a broadening of the distribution due to the additional energy on the system. The most frequently appeared donor–acceptor distance of all H-bonds is around 2.7 Å, which corresponds to the location of the first maximum in the oxygen–oxygen radial distribution functions illustrated in figure 4. Again, we observed that the donor-acceptor distance distribution is insensitive to the methane concentration for the systems studied. Figure 12(a)–(c) show the H-bond angle (hydrogen—donor–acceptor) distribution of all H-bonds for the systems at temperature 270 and 300 K, with methane concentration of 0.643, 0.324 and 0.081 mol/l, respectively. We again find that as temperature increases, there is a broadening of the angle distributions, the most probable angle moves from about 9° at 270 K to 10° at 300 K. We observed the same temperature effect on the H-bond distribution as previous work on the hydrophobic hydration of ethane [19]. The direct comparison of the angle distribution is impossible, as the H-bond angle in [19] was defined as the angle between the O—H bond vector of one water molecule and the O...H H-bond vector between this molecule's H and its near-neighbor's O. Again we found the H-bond angle distribution is independent of the methane concentration.

3.3 Mean square displacement (MSD)

How far will a molecule travel in a given time interval? This matter is relevant to transport processes in the material, such as the rate of diffusion. The average square distance, taken over all molecules, gives us the *mean square displacement* (MSD). As a measure of the average

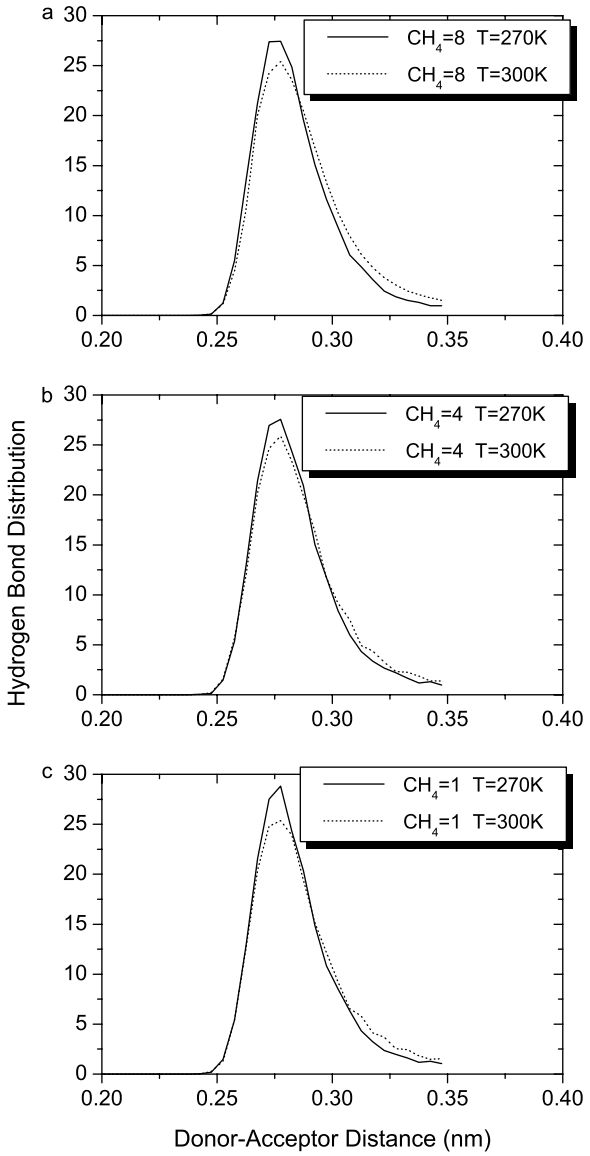

Figure 11. Comparison of the Donor–Acceptor distance distribution of all H-bonds for the systems at temperature 270 and 300 K, with methane concentration of (a) 0.643 mol/l; (b) 0.324 mol/l; (c) 0.081 mol/l.

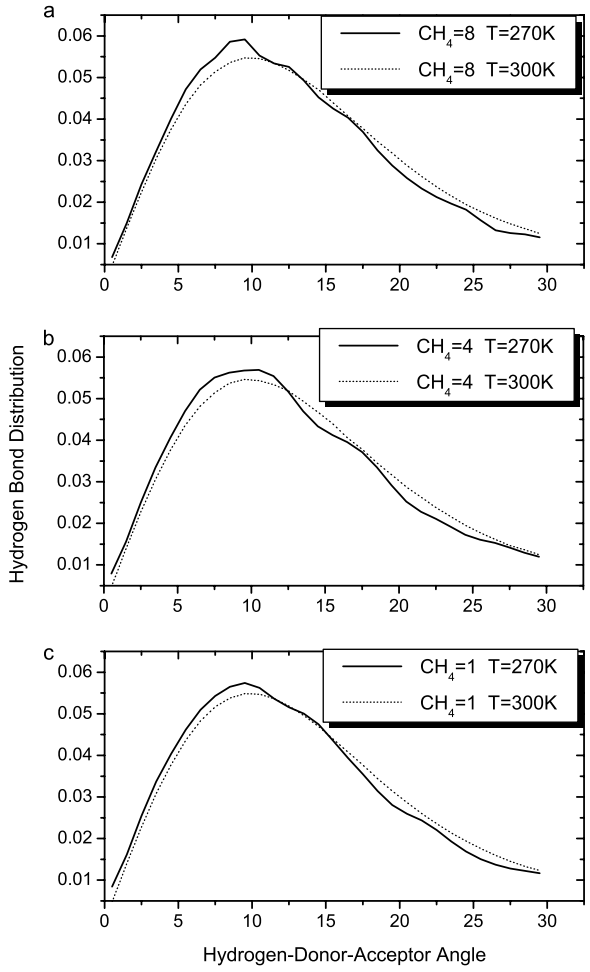

Figure 12. Comparison of the H-bond angle (hydrogen—donor–acceptor) distribution of all H-bonds for the systems at temperature 270 and 300 K, with methane concentration of (a) 0.643 mol/l; (b) 0.324 mol/l; (c) 0.081 mol/l.

distance a molecule travels, it is defined as

$$\mathrm{msd}(t) = \langle \Delta\vec{r}_i(t)^2 \rangle = \langle (\vec{r}_i(t) - \vec{r}_i(0))^2 \rangle$$

where $\vec{r}_i(t) - \vec{r}_i(0)$ is the (vector) distance travelled by molecule i over some time interval of length t, and the squared magnitude of this vector is averaged (as indicated by the angle brackets) over many such time intervals. Often this quantity is averaged also over all molecules in the system, summing i from 1 to N and dividing by N. The limiting slope of msd(t), considered for time intervals sufficiently long for it to be in the linear regime, is related to the self-diffusion constant D,

$$\lim_{t->\infty} \mathrm{msd}(t) = 6\,Dt.$$

Figure 13(a),(b) show the comparison of the MSD of water for the systems with different methane concentration of 0.643, 0.324 and0.081 mol/l, at temperature 270 and 300 K, respectively. The slope of MSD is lower for the system at temperature 270 K, indicating that the water self-diffusion constant D increases as temperature is increased. We observed that an increase in the methane concentration leads to less steep MSD curve, implying less mobility of water molecules.

4. Conclusions

We have performed molecular dynamics simulations of water–methane mixtures at various methane concentrations and temperatures to investigate the diffusion coefficients and the structure of the mixtures at constant NPT ensembles. Our results showed that the methane concentration has little impact on the structure of water and the formation of H-bonds between water molecules. The H-bond numbers, H-bond length and the H-bond angle are independent of the methane concentration at the temperatures and densities examined in this study. However, we also found that the number of H-bonds and angles are sensitive to the temperature. The rise of

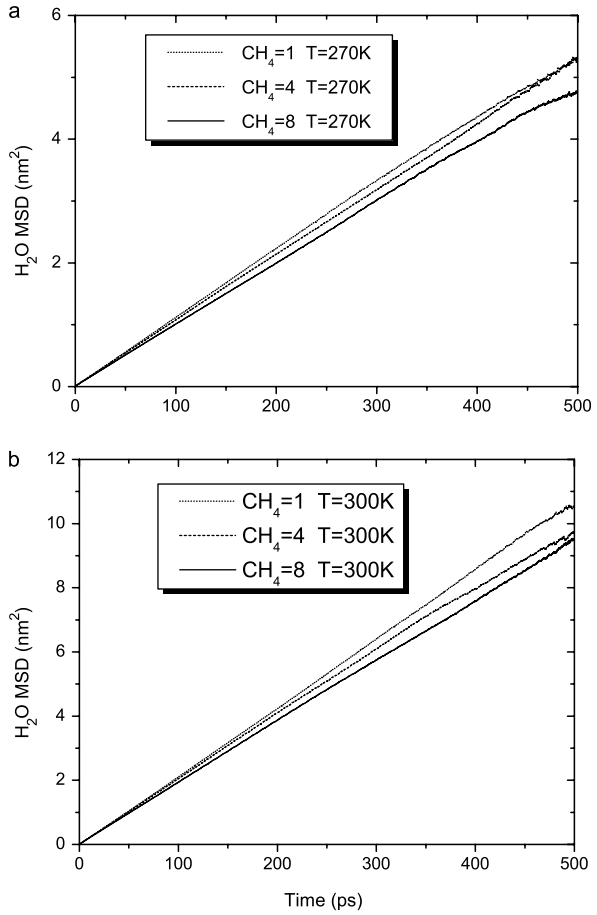

Figure 13. Comparison of the MSD of water for the systems at temperature 270 and 300 K, with different methane concentration. (a) $T = 270$ K; (b) $T = 300$ K.

temperature produces a decrease in the number and an increase in the angle of the H-bonds. Enhanced structuring of the hydration-shell water molecules is indicated by an increase of the first and second peak in the water oxygen–oxygen radial distribution function as temperature is decreased. Self diffusion coefficient of water is sensitive to the methane concentration and temperature.

Acknowledgements

Junfang Zhang thanks CSIRO for providing a postdoctoral fellowship. The authors thank Ronald Blaak and Yang Ye for their support in using GROMACS during the course of this work.

References

[1] W.L. Jorgensen, J. Chandrasekhar, J.D. Madura. Comparison of simple potential functions for simulating liquid water. *J. Chem. Phys.*, **79**, 926 (1983).
[2] Z. Cao, J.W. Tester, K.A. Sparks, B.L. Trout. Molecular computations using robust hydrocarbon–water potentials for predicting gas hydrate phase equilibria. *J. Phys. Chem. B*, **105**, 10950 (2001).
[3] P.M. Rodger. Stability of gas hydrates. *J. Phys. Chem.*, **94**, 6080 (1990).
[4] M.T. Storr, P.C. Taylor, J.-P. Monfort, P.M. Rodger. A new kinetic inhibitor of hydrate crystallisation. *J. Am. Chem. Soc.*, **126**, 1569 (2004).
[5] E.D. Sloan. *Clathrate Hydrates of Natural Gases*, 2nd ed., Dekker, New York, NY (1998).
[6] C.A. Koh. Towards a fundamental understanding of natural gas hydrates. *Chem. Soc. Rev.*, **31**, 157 (2002).
[7] N.J. English, J.K. Johnson. Molecular-dynamics simulations of methane hydrate dissociation. *J. Chem. Phys.*, **123**, 244503 (2005).
[8] N.T. Skipper. Evidence for a temperature-dependent hydrophobic attraction. *Chem. Phys. Lett.*, **207**, 424 (1993).
[9] P.L. Chau, R.L. Mancera. Computer simulation of the structural effect of pressure on the hydrophobic hydration of methane. *Mol. Phys.*, **96**, 109 (1999).
[10] E. Lindahl, B. Hess, D. van der Spoel. A package for molecular simulation and trajectory analysis. *J. Mol. Model*, **7**, 306 (2001).
[11] H.J.C. Berendsen, D. van der Spoel, R. van Drunen. GROMACS: a message-passing parallel molecular dynamics implementation. *Comput. Phys. Comm.*, **91**, 43 (1995).
[12] http://www.gromacs.org
[13] T. Darden, D. York, L. Pedersen. Particle mesh Ewald: an $N\log(N)$ method for Ewald sums in large systems. *J. Chem. Phys.*, **98**, 10089 (1993).
[14] U. Essmann, L. Perera, M.L. Berkowitz, T. Darden, H. Lee, L.G. Pedersen. A smooth particle mesh Ewald method. *J. Chem. Phys.*, **103**, 8577 (1995).
[15] J.-P. Ryckaert, G. Ciccotti, H.J.C. Berendsen. Numerical integration of the Cartesian equations of motion of a system with constraints: molecular dynamics of *n*-alkanes. *J. Comp. Phys.*, **23**, 327 (1977).
[16] H.J.C. Berendsen, J.P.M. Postma, W.F. van Gunsteren, A. Dinola, R. Haak. Molecular dynamics with coupling to an external bath. *J. Chem. Phys.*, **81**, 3684 (1984).
[17] S. Nishimura, S. Biggs, P.J. Scales, T.W. Healy, K. Tsunematsu, T. Tateyama. Molecular-scale structure of the cation modified muscovite mica basal plane. *Langmuir*, **10**, 4554 (1994).
[18] N.T. Skipper. Computer simulation of methane–water solutions. Evidence for a temperature-dependent hydrophobic attraction. *Chem. Phys. Lett.*, **207**, 424 (1993).
[19] R.L. Mancera, A.D. Buckingham. Temperature effects on the hydrophobic hydration of ethane. *J. Phys. Chem.*, **99**, 14632 (1995).